AJNR

MR evaluation of vertebral metastases: T1-weighted, short-inversion-time inversion recovery, fast spin-echo, and inversion-recovery fast spin-echo sequences.

R C Mehta, M P Marks, R S Hinks, G H Glover and D R Enzmann

AJNR Am J Neuroradiol 1995, 16 (2) 281-288
http://www.ajnr.org/content/16/2/281

MR Evaluation of Vertebral Metastases: T1-weighted, Short-Inversion-Time Inversion Recovery, Fast Spin-Echo, and Inversion-Recovery Fast Spin-Echo Sequences

Rahul C. Mehta, Michael P. Marks, R. Scott Hinks, Gary H. Glover, and Dieter R. Enzmann

PURPOSE: To compare the detectability of vertebral metastatic disease on T1-weighted, short-inversion-time inversion recovery (STIR), fast spin-echo (FSE), fat-saturated FSE, and inversion recovery FSE (IRFSE) MR sequences using percent contrast and contrast-to-noise ratios. **METHODS:** Patients with proved metastatic disease underwent imaging on a 1.5-T MR system with sagittal T1-weighted (800/20/2 [repetition time/echo time/excitations]) (91 patients), STIR (1400/43/2; inversion time, 140) (91 patients), FSE (4000/180/2) (46 patients), fat-saturated FSE (4000/180/2) (16 patients), and IRFSE (29 patients) sequences. Percent contrast and contrast-to-noise ratio were calculated for the lesions. The number of metastatic lesions detected with each of the pulse sequences was also calculated. **RESULTS:** Mean percent contrast was, for T1-weighted sequence, −42.2 ± 1%; STIR, 262 ± 34%; FSE, 121 ± 21%; fat-saturated FSE, 182 ± 6%; and IRFSE, 272 ± 47%. The mean contrast-to-noise ratio for T1-weighted was −4.63 ± 1.7; STIR, 10.8 ± .98; FSE, 4.16 ± .76; fat-saturated FSE, 4.87 ± .19; and IRFSE, 5.2 ± .87. STIR and IRFSE showed the highest number of lesions, followed by T1-weighted, fat-saturated FSE, and FSE sequences. T1-weighted sequences showed 94%, FSE 55%, and fat-saturated FSE 78% of the lesions detected. Epidural metastatic lesions were better depicted on T1-weighted, FSE, and fat-saturated FSE sequences. **CONCLUSION:** STIR was superior to both T1-weighted and FSE (with and without fat saturation) for detection of metastatic lesions, in terms of both percent contrast and contrast-to-noise ratio and visibility. IRFSE was equal to STIR for the detection of metastasis by both subjective and objective criteria. T1-weighted, FSE, and fat-saturated FSE sequences were superior to STIR and IRFSE in the detection of epidural metastatic disease. IRFSE provided faster scanning time, which could be translated into greater resolution.

Index terms: Spine, neoplasms; Spine, magnetic resonance; Magnetic resonance, comparative studies

AJNR Am J Neuroradiol 16:281–288, February 1995

Vertebral metastases occur in 10% of all patients with malignant neoplasms and account for 39% of all skeletal metastases (1). Detection of metastatic disease in the vertebral bodies is important for appropriate treatment of patients with known malignant neoplasms. In addition, spinal metastatic deposits cause cord or nerve root compression, resulting in neurologic deficits that can significantly alter the course and treatment of a patient's disease.

Traditional imaging methods including radionuclide scintigraphy, myelography, and computed tomography, performed alone or together, may be inadequate for determining the extent of the metastatic disease. Magnetic resonance (MR) is sensitive to the detection of marrow changes in metastatic disease and its contributions to the detection and assessment of spinal metastatic disease have been described previously (2–13).

The short-inversion-time inversion recovery (STIR) pulse sequence has a high sensitivity for the detection of neoplasia because of its ability

Received August 18, 1993; accepted after revision July 14, 1994.

From the Department of Radiology, Stanford University Medical Center, Stanford, Calif (R.C.M., M.P.M., G.H.G., D.R.E.); and GE Medical Systems, Milwaukee, Wisc (R.S.H.).

Address reprint requests to Dieter R. Enzmann, MD, Department of Radiology, Room S-072, Stanford University Medical Center, Stanford, CA 94305-5105.

AJNR 16:281–288, Feb 1995 0195-6108/95/1602–0281

to show the combined effects of prolonged T1 and T2 relaxation times of these pathologic tissues (3, 8, 14). By choosing the appropriate inversion time, fat can effectively be suppressed, an important feature in imaging the spine because of marrow fat within the vertebrae. Suppression of marrow fat is important to detection of metastatic lesions in the spine, because subtle low-intensity lesions can be obscured by the high signal intensity of marrow fat on routine T1-weighted spin-echo imaging. This is important because vertebral metastases are common in the elderly population with fatty vertebral marrow. When a longer repetition time (1400 to 2000 milliseconds) is used, in combination with multiple excitation (to improve signal-to-noise), this sequence requires approximately 7 minutes to complete, even at low resolution (256 × 128 matrix, 128 phase-encoding steps).

Fast spin-echo (FSE) samples k-space more efficiently than conventional spin-echo imaging (Fram EK, Keller PJ, Drayer BP, "Rapid Spin Echo Imaging [RARE] Producing Two Effective Echo Times by Sharing Views," abstract, Society for Magnetic Resonance in Medicine, 1991; 218) (15–19). FSE imaging may have a potential role in evaluating spinal metastatic disease, when T2-weighted sequences are appropriate. The inversion-recovery FSE (IRFSE) sequence has the potentially attractive features of STIR sensitivity, in combination with increased resolution (512 × 256 matrix, 256 phase-encoding steps) and rapid scanning time (2 minutes, 8 seconds).

This study was designed to compare prospectively FSE, fat-saturated FSE, and IRFSE with conventional spin-echo, T1-weighted, and STIR imaging.

Subjects and Methods

Ninety-one consecutive patients (47 female and 44 male) between the ages of 5 and 87 years (mean age, 58.76 years) with known primary tumors and proved vertebral metastases (documented on multiple modalities; ie, correlation with bone scintigraphy and progression on serial MR exams) were imaged over a 6-month period. A total of 125 spinal MR examinations (19 cervical, 52 thoracic, and 54 lumbar) were performed prospectively. All patients were scanned on a 1.5-T MR imaging unit, using the multiphase array coil, 24-cm field-of-view for cervical and 36-cm field-of-view for thoracic and lumbar spine, and 5-mm thin sections with 0.5-mm intersection spacing. The echo train length of 8 and bandwidth of 16 MHz was used for the FSE, fat-saturated FSE, and IRFSE sequences. The echo spacing was 20 milliseconds for FSE, fat-saturated FSE, and IRFSE. The actual and effective echo time was the same, 180 milliseconds; because of a straight phase-encode ordering, the effective echo time was at the center of the echo train length. The distribution of primary neoplasms is shown in Table 1.

TABLE 1: Site of primary tumor

Primary	Number
Breast	22
Lung	14
Prostate	11
Multiple myeloma	8
Lymphoma/leukemia	6
Osteosarcoma/Ewing	4
Rhabdomyosarcoma	3
Melanoma	3
Head/neck	3
Colon	3
Pancreatic	2
Neuroblastoma	1
Primitive neuroectodermal tumor	1
Malignant giant cell tumor	1
Renal	1
Thyroid	1
Unknown (all adenocarcinomas)	7
Total	**91**

Three sequential studies of groups of sequences were performed in the study population. All three study groups had spin-echo sagittal and axial T1-weighted and STIR imaging. These two pulse sequences were compared sequentially with FSE (group 1), fat-saturated FSE (group 2), and IRFSE (group 3). There were 46 patients in group 1, 16 in group 2, and 29 in group 3. The sequential groupings reflected the sequential availability of the different FSE pulse sequences. All scans were obtained in the sagittal plane to compare all pulse sequences for the entire study population. The parameters for each pulse sequences were as follows for each of the groups: T1-weighted, 800/20/2 (repetition time/echo time/excitations) (512 × 256 matrix; scanning time, 6 minutes, 35 seconds); STIR, 1400/43/2 (inversion time, 140; 256 × 128 matrix; scanning time, 6 minutes, 58 seconds); FSE, 4000/180/2 (256 × 256 matrix; scanning time, 2 minutes, 8 seconds); fat-saturated FSE, 4000/180/2 (256 × 256 matrix; scanning time, 2 minutes, 8 seconds); and IRFSE, 4000/52/140/2 (512 × 256 matrix; scanning time, 2 minutes, 8 seconds). One fat saturation on FSE was achieved by applying a frequency-selective saturation pulse. A 512 × 256 matrix was used for T1-weighted and IRFSE sequences. All the sequences had 256 phase-encoding steps except STIR (the use of 256 phase-encoding steps in a 256 × 256 matrix in STIR would result in a prohibitively long 13-minute scan).

The percent contrast and contrast-to-noise ratio were calculated by placing operator-determined regions of interest within the metastatic lesions, in normal marrow and

in air for each pulse sequence. Three randomly selected lesions in each patient were measured for each of the three pulse sequences. The mean percent contrast and contrast-to-noise ratio were calculated for all the lesions for each of the sequences. Tests for statistical significance (two-tailed t test) were applied. Air measurements were obtained along the phase-encoding direction in areas adjacent to the spine. The same regions of interest were used for each sequence in all patients. The percent contrast (%C) and contrast-to-noise ratio (CNR) were calculated by the following formulas:

$$\%C = \frac{SI(lesion) - SI(back)}{SI(back)} \times 100$$

$$CNR = \frac{SI(lesion) - SI(back)}{noise}$$

$$Noise = \frac{SI(air)}{\sqrt{\pi}}$$

where SI indicates signal intensity and (back), background, signal intensity of normal marrow.

The scans were also reviewed qualitatively by two neuroradiologists and scored by consensus to determine the visual detectability of the metastatic lesions for each of the pulse sequences. A forced-choice classification for each lesion was made, placing each into one of three categories: (*a*) metastatic lesions well seen and seen to the same extent; (*b*) lesions faintly seen or seen to a lesser extent; and (*c*) lesions not seen and isointense to the normal marrow.

Results

Group 1: T1-weighted, STIR, and FSE

This group included 46 patients who underwent T1-weighted, STIR, and FSE sequences in the sagittal plane (Fig 1). Table 2 shows the percent contrast and contrast-to-noise ratio calculated for the metastatic lesions for each of the three pulse sequences. The STIR sequence showed a much greater percent of contrast and contrast-to-noise ratio for metastatic lesions than T1-weighted spin-echo or FSE sequences ($P < .001$). Table 3 shows the lesion detection rate for the three pulse sequences. STIR detected far more lesions than either the T1-weighted or FSE pulse sequences. In addition, 35 lesions on T1-weighted and 46 lesions on the FSE sequence were not as well seen as on STIR.

Group 2: T1-weighted, STIR, and Fat-saturated FSE

This group consisted of 16 patients evaluated with T1-weighted, STIR, and fat-saturated

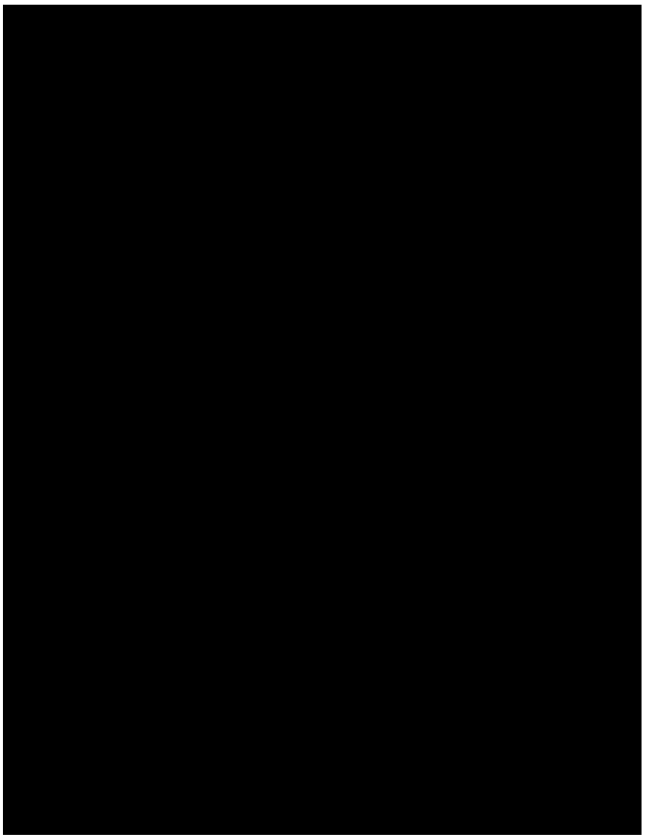

Fig 1. A 43-year-old patient with breast carcinoma widely metastatic to thoracic spine.

A, Sagittal T1-weighted image of thoracic spine shows multiple low-intensity lesions within the vertebrae.

B, Sagittal STIR confirms the presence of multiple lesions, seen here as high-signal-intensity foci within the marrow.

C, Sagittal FSE depicts the lesions poorly with some lesions appearing isointense to the marrow and others appearing low signal intensity when compared with the signal of the marrow.

TABLE 2: Percent contrast (%C) and contrast-to-noise ratio (CNR) of T1-weighted, STIR, and FSE sequences

Pulse Sequence	%C, mean ± SEM	CNR, mean ± SEM
T1	−21.08 ± 6%	−4.63 ± 1.7
STIR	459 ± 52%	10.8 ± 0.98
FSE	121 ± 21%	4.16 ± 0.76

TABLE 3: Subjective detection and grading of lesions on T1-weighted, STIR, and FSE sequences

STIR, total lesions	FSE			T1-Weighted		
	Equal to STIR	Less than STIR	Not Seen	Equal to STIR	Less than STIR	Not Seen
197	62	46	89	147	35	15

Note.—Equal to STIR indicates extent of the lesion same as that on STIR; less than STIR, diameter of the lesion not more than 50% of that seen on STIR; and not seen, lesion isointense to the marrow and not visible.

FSE sequences (Fig 2). The percent contrast and contrast-to-noise ratios are tabulated in Table 4. The STIR sequence showed a much greater percent contrast and contrast-to-noise ratio for metastatic lesions compared with T1-weighted spin-echo or fat-saturated FSE sequences ($P < .001$). The percent contrast and contrast-to-noise ratio were highest for STIR (262% ± 9% and 15 to 3 ± 0 to 56, respectively). The addition of fat saturation to FSE improved the percent contrast and contrast-to-noise ratio when compared with FSE without fat saturation. Of the 65 lesions seen on STIR, 24 on fat-saturated FSE were seen to the same extent as on STIR, 27 lesions were seen to a lesser extent, and 14 lesions were not seen at all (ie, were isointense to the marrow) (Table 5).

TABLE 4: Percent contrast (%C) and contrast-to-noise ratio (CNR) of T1-weighted, STIR, and fat-saturated FSE sequences

Method	%C, mean ± SEM	CNR, mean ± SEM
T1	−42 ± 1%	−12.5 ± 0.56
STIR	262 ± 9%	15.3 ± 0.56
Fat-saturated FSE	182 ± 6%	4.87 ± 0.19

Group 3: T1-weighted, STIR, and IRFSE

The 29 patients in this group were evaluated with T1-weighted, STIR, and IRFSE sequences (Figs 3 and 4). IRFSE had the highest percent contrast; 275% ± 47%, and contrast-to-noise ratio was 5.2 ± 0.87. The IRFSE was comparable to the STIR sequence, both in percent contrast and contrast-to-noise ratio (Table 6) ($P <$ .001). In addition, visual grading of the lesions shows that all 196 lesions seen on STIR were detected to the same extent on IRFSE (Table 7).

Epidural Disease

Seven patients in the study group had epidural extension of tumor documented on MR imaging. The presence of epidural extension of the tumor was better depicted in all seven cases with the T1-weighted and FSE pulse sequences (three FSE, four fat-saturated FSE). In these cases, epidural lesions had a lower signal intensity than cerebrospinal fluid (CSF) and were clearly depicted as separate from CSF. The STIR sequence, on the other hand, depicted these metastatic lesions as a high signal intensity similar to that of CSF, causing the lesion to be obscured (Fig 5).

Fig 2. A 67-year-old patient with breast cancer metastatic to the cervical spine.

A, Sagittal T1-weighted image of cervical spine shows low-intensity metastatic lesions within the vertebral bodies of C-2, C-5, C-6, and T-2.

B, Sagittal STIR confirms the presence of multiple lesions, seen here as high-signal-intensity foci within the marrow of these vertebrae; in addition there is a subtle increase in marrow signal of C-3 and C-4, indicating early metastatic disease (compare them with the lower signal of marrow on STIR in C-6 and C-7).

C, Sagittal fat-saturated FSE depicts the lesions poorly. Also the involvement of the posterior elements of C-2, C-5, and C-6 are poorly seen as compared with STIR.

TABLE 5: Subjective detection and grading of lesions on T1-weighted, STIR, and fat-saturated FSE sequences

STIR, total lesions	Fat-saturated FSE			T1-Weighted		
	Equal to STIR	Less than STIR	Not Seen	Equal to STIR	Less than STIR	Not Seen
65	24	27	14	57	6	2

Note.—Equal to STIR indicates extent of the lesion same as that on STIR; less than STIR, diameter of the lesion not more than 50% of that seen on STIR; and not seen, lesion isointense to the marrow and not visible.

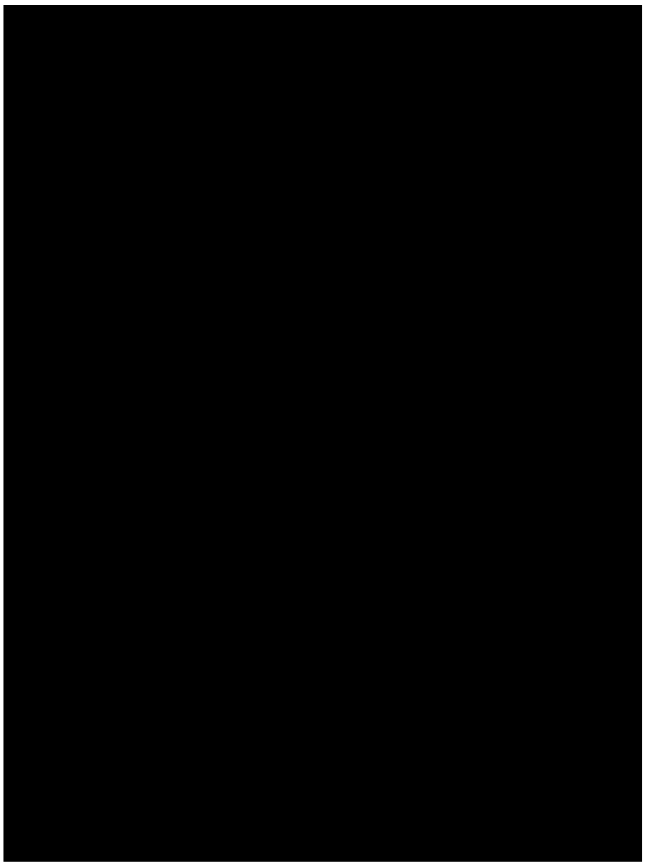

Fig 3. A 77-year-old patient with widely disseminated lymphoma.

A, Sagittal T1-weighted image shows diffuse replacement of vertebral marrow by metastatic deposits.

B, Sagittal STIR and *C*, sagittal IRFSE show the low-signal-intensity lesions on T1-weighted images as high-signal-intensity metastatic lesions throughout the thoracolumbar spine. The remaining normal fatty marrow in T-12, L-1, and L-2 is seen as a very low, dark-appearing region within the vertebra.

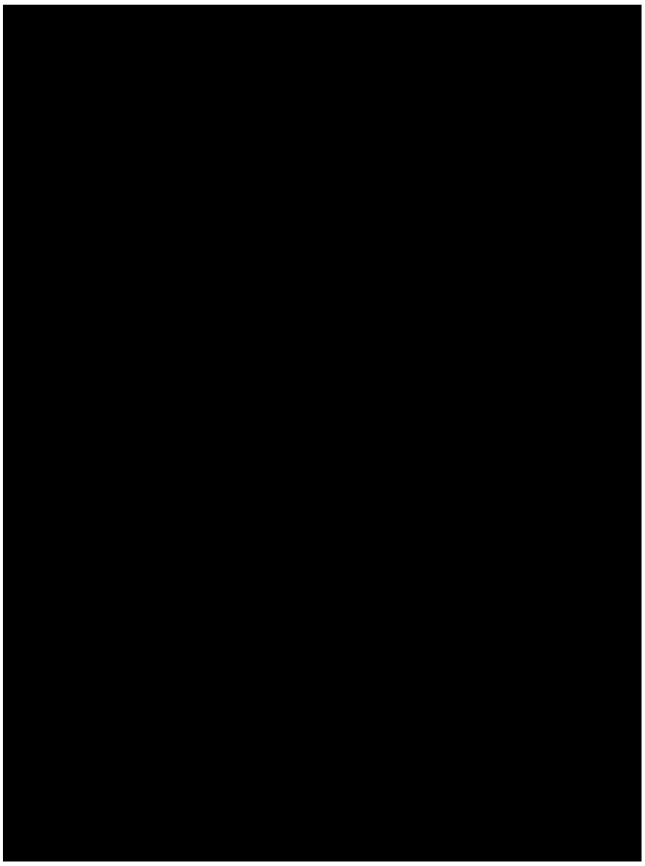

Fig 4. A 48-year-old patient with widely metastatic carcinoma unknown primary.

A, Sagittal T1-weighted image shows diffuse replacement of vertebral marrow fat by the metastatic deposits.

B, Sagittal STIR and *C*, sagittal IRFSE confirm the widespread disease in the lower thoracic and lumbar spine. Note that the metastases appear almost equal in signal intensity and extent. There is diffuse marrow replacement as compared with the normal appearance of the vertebrae in 3B and C.

Discussion

In a patient with neoplastic disease, MR is usually performed to detect metastatic disease to the vertebrae, nerve root, and spinal cord compression. This means it has to distinguish tumor from normal bone marrow. The interpretation of the results of this study depends on the understanding of the appearance of marrow neoplastic disease on short-repetition-time/short-echo-time (T1-weighted) spin-echo and inversion-recovery images. The normal vertebra in young adults is composed primarily of hemopoietic bone marrow containing significant amounts of fat (from 25% to 50%). With aging, the marrow is converted to even larger amounts of fat, and correspondingly the mean percent volume of hematopoietic marrow de-

TABLE 6: Percent contrast (%C) and contrast-to-noise ratio (CNR) of T1-weighted, STIR, and IRFSE sequences

Method	%C, mean ± SEM	CNR, mean ± SEM
T1	−42 ± 1%	−12.5 ± 0.56
STIR	262 ± 34	9.5 ± 1.17
IRFSE	275 ± 47%	5.2 ± 0.87

TABLE 7: Subjective detection and grading of lesions on T1-weighted, STIR, and IRFSE sequences

STIR, total lesions	IRFSE	T1-Weighted		
	Equal to STIR	Equal to STIR	Less than STIR	Not Seen
196	196	163	22	11

Note.—Equal to STIR indicates extent of the lesion same as that on STIR; less than STIR, diameter of the lesion not more than 50% of that seen on STIR; and not seen, lesion isointense to the marrow and not visible.

creases progressively, with the result that in the eighth decade of life it is about half of that present in the first decade (29.2% versus 57.9%) (20, 21). Therefore, the signal intensity of the vertebrae on T1-weighted images in younger patients is lower than that of older patients, a factor reflecting the higher percentage hemopoietic marrow in this younger age group. At a field strength of 1.5 T, the marrow fat of an adult patient provides a near homogenous high signal intensity on T1-weighted images. Metastatic lesions, because of a long T1 relaxation time, are easily detected as low signal intensity within the high-intensity marrow (21, 22). In contrast, STIR and FSE sequences depict tumor as high signal. With this strategy, fat suppression is advantageous to reduce background signal. With STIR sequence, this is achieved by use of the appropriate inversion time. With FSE sequence, this may prove even more important because of the relatively high signal maintained in fat even with a heavily T2-weighted image. Frequency-selective fat suppression therefore can be coupled with FSE. Inversion recovery, or STIR, has the highest contrast between tumor and normal marrow of all these pulse sequences. It depicts the disease as a focus of high signal intensity against the low-signal fatty marrow (22, 23).

STIR sequences offer two advantages in the assessment of disease replacing the bone marrow. First, it is possible to suppress the signal from fat using an inversion time that is 0.56 to 0.69 of the T1 of that tissue, provided the repetition time is greater than 3T1. With the T1 relaxation time of fat approximately 200 milliseconds, the signal intensity from the fat is suppressed on STIR images with an inversion time in the range of 100 to 150 milliseconds. Second, the effects of prolonged T1 and T2 relaxation times are potentiated in STIR sequences. Pathologic conditions typically have prolonged T1 and T2 relaxation times, and the additive effect of these two parameters results in high signal intensity.

The STIR sequence (both spin-echo and FSE versions) had significantly higher percent contrast and contrast-to-noise ratios as compared with the other sequences, T1-weighted, FSE,

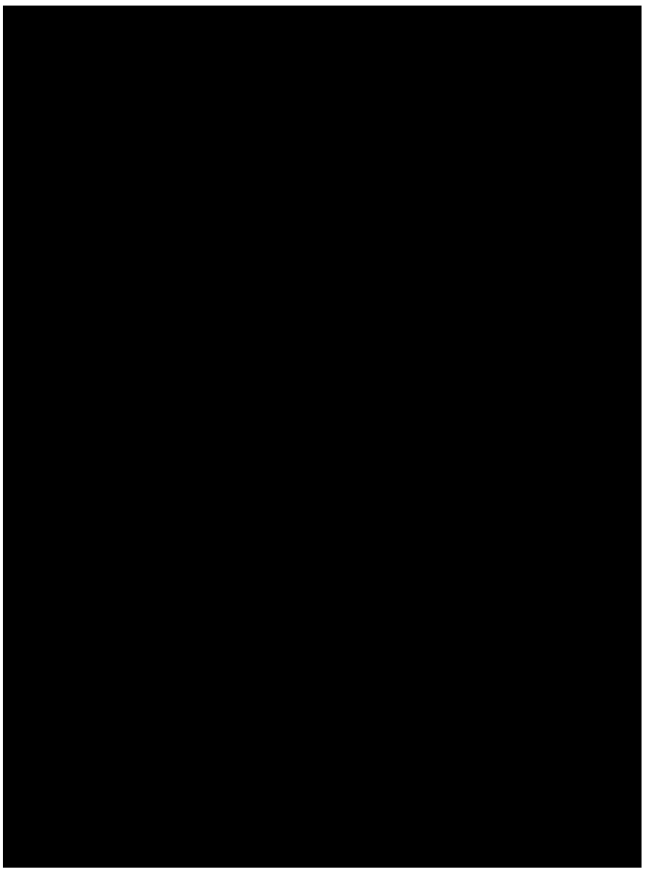

Fig 5. A 35-year-old patient with lymphoma.

A, Sagittal T1-weighted image of midthoracic spine shows a low-signal-intensity lesion at T-8 with epidural extension. In addition, note the invasion of T-10 and T-11 vertebrae anteriorly by the retroperitoneal nodes.

B, Sagittal STIR shows the metastatic deposits as high-signal lesions at T-8, T-10, and T-11, but the epidural tumor is eclipsed by the high-signal CSF.

C, FSE shows the epidural tumor well because of high signal intensity of the CSF but low signal of the tumor. In absence of the epidural tumor, the metastasis at T-8 would be difficult to detect because of poor contrast with the marrow fat.

and fat-saturated FSE (two-tailed t test; STIR versus FSE, $P < .001$; STIR versus fat-saturated FSE, $P < .001$). There was no statistical difference in the percent contrast or contrast-to-noise ratio between STIR and IRFSE. The improved depiction of lesions with STIR was also confirmed by the detection rate of the lesions. In group 1, for example, 50 (25.4%) foci of disease out of 197 were not depicted on T1 images. This is an unacceptably high rate of failure to detect metastatic disease. The STIR sequence was also superior to the FSE (group 1) in percent contrast and contrast-to-noise ratio. Not only did FSE fail to show approximately 89 (45.2%) of 197 lesions, but even in many cases those shown on FSE were not shown to the same extent as lesions depicted with STIR. Moreover, the metastatic lesions could be isointense to normal marrow and not detected at all. A review of the 11 patients in whom the FSE sequence completely missed the lesions revealed that location and the cell type of the primary tumor did not correlate with this detection failure. The causes of such sporadic low signal of metastatic sites are indeterminate. There was some improvement in the detection rate as well as the percent contrast and contrast-to-noise ratios by the addition of fat saturation in the FSE sequence. However, STIR still proved to be superior. Inversion-recovery FSE was the only variant of FSE which was, objectively and subjectively, comparable to STIR images. Thus, our results differ from those of a recently published study (24), which found metastatic lesions more conspicuous on the fat-saturated T2-weighted sequence as compared with an IRFSE sequence, although there was no statistical difference in the contrast-to-noise ratios. A drawback of STIR and IRFSE is their failure to show epidural metastatic disease, because the CSF and the epidural tumor both have a high signal intensity and the metastatic disease, which appeared isointense with CSF, is thus silhouetted. FSE and fat-saturated FSE were superior however for the detection of epidural metastatic disease because of the low signal intensity of the tumor as compared with the high signal intensity of the CSF. T1-weighted images were also superior to STIR and IRFSE because of the different signal intensities of the tumor and CSF (Fig 5). This drawback of STIR and IRFSE was offset by the routine performance of the axial T1-weighted sequence through the lesions.

An intriguing problem that developed during the study was the fall in percent of contrast and contrast-to-noise ratio of STIR in group 3. The study population in group 1 was not significantly different from subgroups 2 and 3 in terms of the primary malignancies or age. After we completed the first phase of the study, the MR scanners at our institution underwent a software and hardware update for the introduction of the FSE and IRFSE sequences. We have consulted researchers working with FSE, fat-saturated FSE, and IRFSE at two other sites, and their experience has been similar. The technical problems affecting STIR are likely to influence both spin-echo STIR and FSE STIR, and therefore we believe that the relative results of our study (STIR being equal to IRFSE) are still valid. We are pursuing the cause of the decline in contrast with STIR.

We have now included IRFSE in our protocol for imaging of vertebral metastatic disease. Since then, our average scanning time has decreased without any compromise in terms of percent contrast and contrast-to-noise ratios. This has also benefited the patients with metastatic disease in terms of pain and discomfort, because they have to spend less time on the scanner.

In conclusion, we think that the most effective protocol for MR imaging of vertebral metastatic disease includes a STIR sequence. The IRFSE sequence has a significant advantage, because it has a shorter scan time compared with the conventional STIR sequence. This time saving would allow for the selection of parameters that give greater resolution, such as selection of large (512×256) matrix size.

References

1. McNeil BJ. Value of bone scanning in neoplastic disease. *Semin Nucl Med* 1984;14:277–286
2. Avrahami E, Tadmor R, Dally O, Hadar H. Early MR demonstration of spinal metastases in patients with normal radiographs and CT and radionuclide bone scans. *J Comput Assist Tomogr* 1989; 13(4):598–602
3. Stimac GK, Porter BA, Olson DO, et al. Gadolinium-DTPA-enhanced MR imaging of spinal neoplasms: preliminary investigation and comparison with unenhanced spin-echo and STIR sequences. *AJNR Am J Neuroradiol* 1988;9:839–846
4. Carmody RF, Yang PJ, Seeley GW, et al. Spinal cord compression due to metastatic disease: diagnosis with MR imaging versus myelography. *Radiology* 1989;173:225–229
5. Yuh WTC, Zachar CK, Barloon TJ, et al. Vertebral compression fractures: distinction between benign and malignant causes with MR imaging. *Radiology* 1989;172:215–218

6. Smith SR, Williams CE, Davies JM, Edwards RHT. Bone marrow disorders: characterization with quantitative MR imaging. *Radiology* 1989;172:805–810
7. Smoker WRK, Goderdky JC, Knutson RK, et al. The role of MR imaging in evaluating metastatic spinal disease. *AJNR Am J Neuroradiol* 1987;8:901–908
8. Feckenstein JL, Archer BT, Barker BA, et al. Fast short-tau inversion-recovery MR imaging. *Radiology* 1991;179:99–504
9. Baker LL, Goodman SB, Perkash I, et al. Benign versus pathologic compression fractures of vertebral bodies: assessment with conventional spin-echo, chemical-shift, and STIR MR imaging. *Radiology* 1990;174:495–502
10. Blews DE, Wang H, Kumar AJ, et al. Intradural spinal metastases in pediatric patients with primary intracranial neoplasms: Gd-DTPA enhanced MR vs CT myelography. *J Comput Assist Tomogr* 1990;14(5):730–735
11. Weiner SN, Neumann DR, Rzeszotarski MS. Comparison of magnetic resonance imaging and radionuclide bone imaging of vertebral fractures. *Clin Nucl Med* 1989;9:666–670
12. Godersky JC, Smoker WRK, Knutson RK. Use of magnetic resonance imaging in the evaluation of metastatic spinal disease. *Neurosurgery* 1987;21:676–680
13. Mehta RC, Wilson MA, Perlman SB. False negative bone scan in extensive metastatic disease: CT and MR findings. *J Comput Assist Tomogr* 1989;13(4):717–719
14. Rahmouni A, Divine M, Mathieu D, et al. Detection of multiple myeloma involving the spine: efficacy of fat suppression and contrast enhanced MR imaging. *AJR Am J Roentgenol* 1993;160: 1049–1052
15. Hennig J, Naureth A, Freidburg H. RARE imaging: A fast imaging method for clinical MR. *Magn Reson Med* 1986;3:823–833
16. Hennig J, Freidburg H. Clinical applications and methodological developements of the RARE technique. *Magn Reson Med* 1988; 6:391–395
17. Mulkern RV, Wong STS, Winalski C, Jolsez FA. Contrast manipulation and artifact assessment of 2D and 3D RARE sequences. *Magn Reson Imaging* 1990;8:557–566
18. Mielki P, Mulkern RV, Panych LP, Jolsez FA. Comparing FAISE method with conventional dual-echo sequences. *J Magn Reson Imaging* 1991;1:319–326
19. Constable RT, Smith RC, Gore JC. Signal to noise and contrast in fast spin echo (FSE) and inversion recovery fast spin echo. *J Comput Assist Tomogr* 1992;16(1):41–47
20. Dunhill MS, Anderson JA, Whitehead R. Quantitative histological studies on age changes in bone. *J Pathol Bacteriol* 1967;94:259–291
21. Dooms GC, Fisher MR, Hricak H, et al. Bone marrow imaging: magnetic resonance studies related to age and sex. *Radiology* 1986;155:429–432
22. Bydder GM, Young IR. MR imaging: clinical use of the inversion recovery sequence. *J Comput Assist Tomogr* 1985;9:659–675
23. Dwyer AJ, Frank JA, Sank VJ, et al. Short-T1 inversion-recovery pulse sequence: analysis and initial experience in cancer imaging. *Radiology* 1988;168:827–836
24. Jones KM, Schwartz RB, Mantello MT, et al. Fast spin echo MR in the detection of vertebral metastasis: comparison of three sequences. *AJNR Am J Neuroradiol* 1994;15:401–407


A
B
C

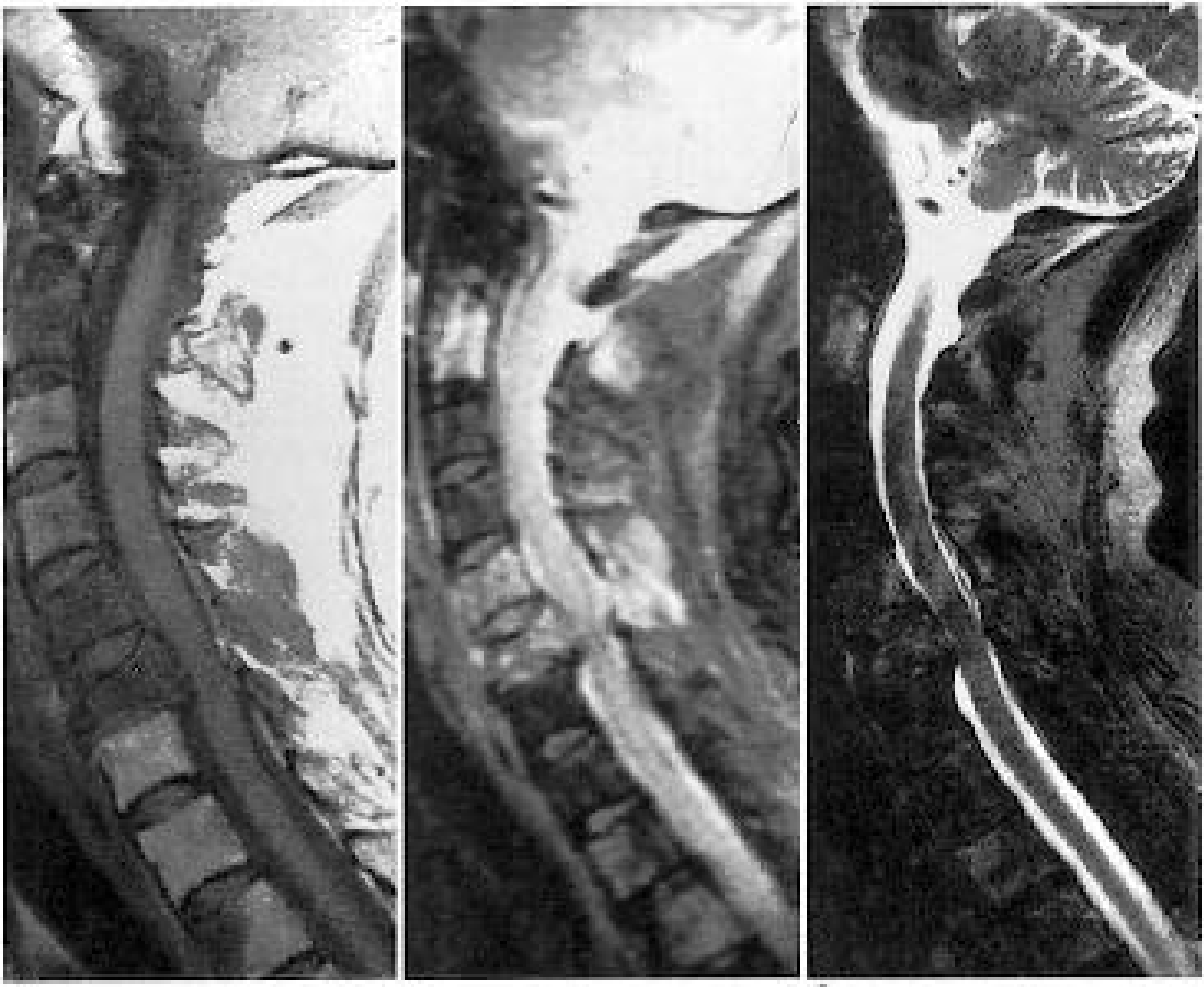
A
B
C

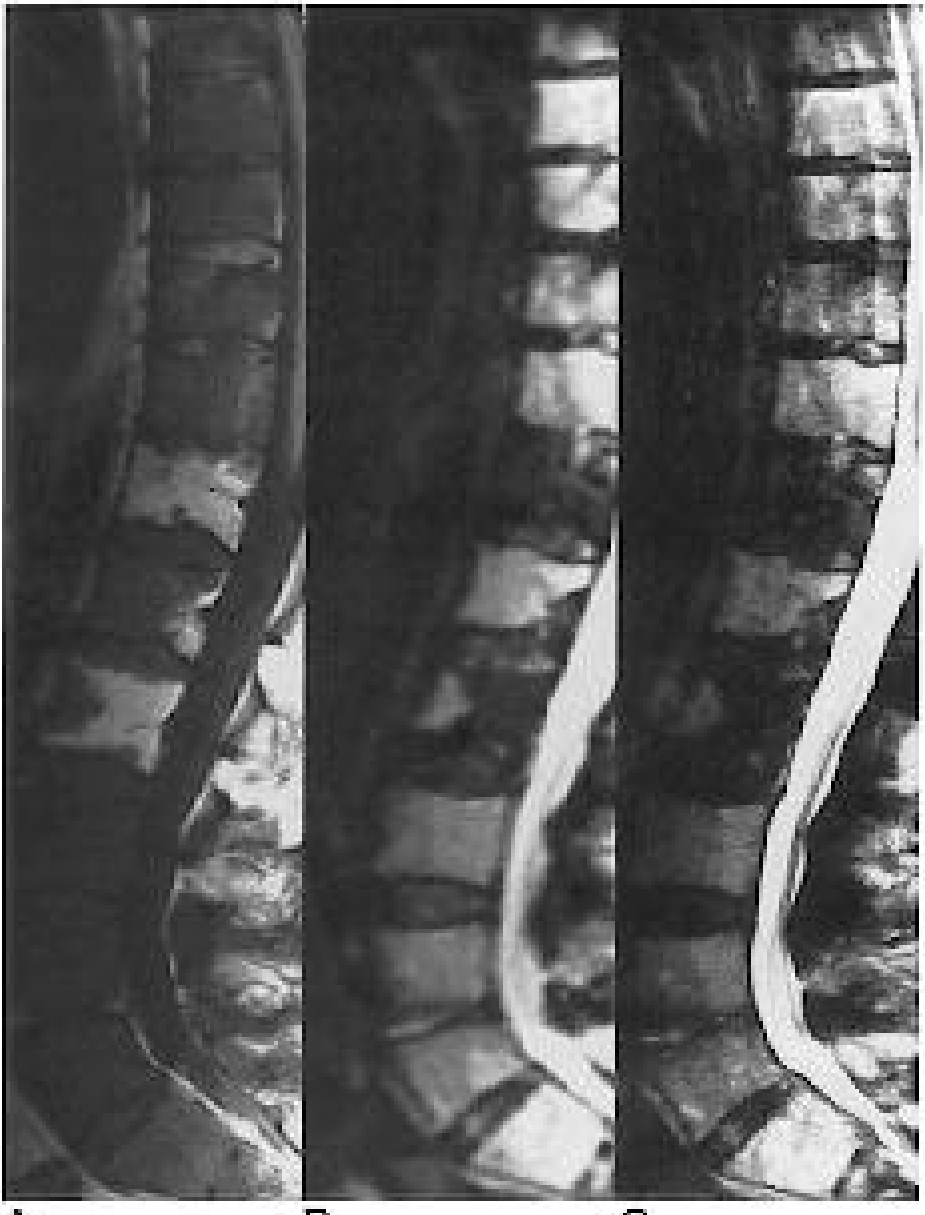
A
B
C


A
B
C

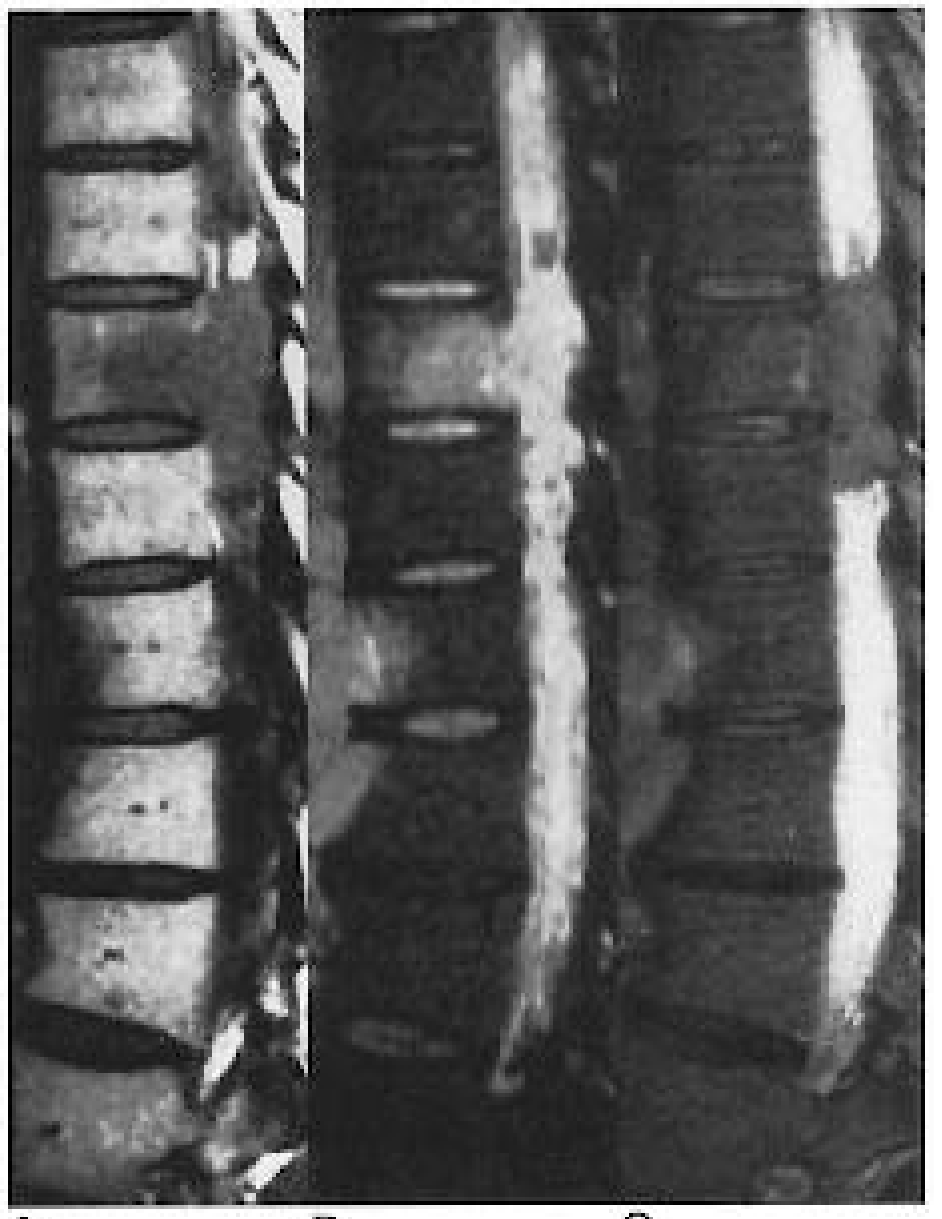

A B C